Available online at www.sciencedirect.com

ScienceDirect

Energy Procedia 59 (2014) 59 – 66

Energy Procedia

European Geosciences Union General Assembly 2014, EGU 2014

Observations of pore pressure in clay-rich materials; implications for the concept of effective stress applied to unconventional hydrocarbons.

Robert Cuss*, Jon Harrington, Caroline Graham, and David Noy

British Geological Survey, Keyworth, Nottingham,NG12 5GG, United Kingdom

Abstract

The concept of effective stress is a well-established relationship where the stress acting on a rock can be viewed as the total stress minus the pore water pressure. In clay-rich rocks this relationship has been seen to be imperfect and a Biot coefficient is added to account for the material properties of the clay matrix. Large, stable pressure differentials and gradients were observed in several argillaceous materials during water and gas injection testing for a number of experimental geometries, including triaxial (Callovo-Oxfordian claystone), shear (kaolinite and Opalinus Clay) and full-scale testing (bentonite). Pore-pressure during water injection appeared to be evenly distributed on the sample scale, whereas in full-scale demonstration a complex distribution was seen, which may partly be due to hydraulic disequilibrium. During gas injection testing all observations suggested that transport was predominantly by dilatancy flow and the formation of micro-fissures. This led to localized pore pressure variations and a complex temporally and spatially varying pore pressure distribution. Isolated pockets of increased gas pressure could be seen to be stable. The nature of pore-pressure distribution, both hydraulic and gaseous, and the stability of pore pressure differentials means that the description of a meaningful average pore pressure was difficult and thus the use of effective stress with a single χ value might misrepresent local stresses within the rock. Localized deformation in the formation of dilatant pathways was dominated by the local gas pressure and not the bulk pore pressure. Therefore the law of effective stress on the micro-scale will be valid, whereas on a bulk scale could lead to errors in model predictions. This also has implications on the release of gas from shale due to the localized influence of stress around a fracture. Flow along fractures was localized with only a proportion of the fracture surface playing a part in both water and gas flow.

Peer-review under responsibility of the Austrian Academy of Sciences

Keywords: Pore pressure; effective stress; shale gas; multi-phase flow; unconventional hydrocarbons.

* Corresponding author. Tel.: +44-115-936-3486; fax: +44-115-936-3200.
E-mail address: rjcu@bgs.ac.uk

Peer-review under responsibility of the Austrian Academy of Sciences
doi:10.1016/j.egypro.2014.10.349

1. Introduction

In a previous paper [1] we introduced a series of observations of pore pressure distributions during multi-phase flow testing of clay-rich rocks. This included tests conducted on Callovo-Oxfordian claystone, kaolinite fault gouge, Opalinus clay and pre-compacted bentonite material. Common features of gas flow and pore pressure distribution were seen between the test materials and at different scales. In this paper, we update the observations made from the different test geometries and discuss these with specific reference to the extraction of unconventional hydrocarbons.

Pore-fluid under pressure has a profound effect on the physical properties of porous solids [2,3]. In a saturated porous system, the fluid supports some proportion of the applied load lowering the overall stress exerted through grains. Strength is therefore determined not by confining pressure alone, but by the difference between confining and pore-pressures:

$$\sigma' = \sigma - \chi u$$

where σ' is effective stress, σ is total stress, and u is pore pressure. Many shale rocks have been shown to follow the law of effective stress, e.g. [4,5]. However, due to the compressibility of clay and the poroelastic effect [6], where the effective stress is modified by the partial transfer of pore-pressure to the granular framework, the law of effective stress is modified with the effective pressure coefficient (χ). Wilcox shale has been shown to have a χ was equal to 0.99 [5], whereas shale for the Mahakam Delta has a χ of 0.65 – 0.85 [7].

Conceptual and numerical models of argillaceous rock deformation, such as critical state soil mechanics [8], use the law of effective stress. Experiments are required to determine the role that pore pressure has on the deformation of sediments. The findings in this paper have implications for our prediction of deformation caused by changes in hydraulic pore pressure during "fracking" and the release of gas as a result of lowering pore pressure within the rock.

2. Experimental geometry 1 – Triaxial testing

The triaxial Stress-Path Permeameter (SPP; [9]) was used to investigate water and gas (helium) flow in Callovo-Oxfordian claystone (COx). The SPP was designed to observe sample volume changes during flow experiments conducted along an evolving stress-path. The test was conducted at a confining pressure of 12.5 MPa, axial load of 13 MPa and a back pressure of 4.5 MPa. The experimental geometry was modified to include two porous stainless-steel annular filter guard-rings 6 mm wide and 2mm deep around the edge of loading platens. The inlet/outlet filter was made up of a porous disc 20 mm in diameter and 2 mm depth. The addition of the guards ring meant that pore pressure was measured at four different points on the test sample providing data on the hydraulic anisotropy and symmetry within the sample.

2.1. Observed pore pressure distribution under in situ stress conditions

Fig. 1a shows the results from a two-step constant head test. Injection pore pressure was raised to 8.5 MPa and then the guard-rings were isolated. Both injection (IGR) and back-pressure (BGR) guard rings showed an initial decrease in pore-pressure, which within a couple of days started to recover in pressure and equilibrated. The IGR stabilized approximately 0.85 MPa below the injection pressure, whereas BGR was about 1.25 MPa above the back pressure. Injection pressure was lowered to 4.5 MPa on Day 98. Over the subsequent remaining time of the stage a slow decrease in pore pressure in IGR and BGR was seen, with BGR decreasing much slower than IGR. The data show that a relatively even distribution in pore pressure was created in the sample. This suggests a relatively evenly distributed pore pressure gradient through the sample. Despite the seemingly even distribution of pore pressure the guard-ring data show pore pressure distribution is not straightforward. The gradient between the guard-rings and injection/back filters is 70.5 $MPa.m^{-1}$ and 104 $MPa.m^{-1}$ at the injection and back-pressure ends of the sample respectively. This difference at the two ends of the sample may be caused by sample anisotropy.

Fig. 1b shows the results from a gas injection test. BGR pressure showed little change during the first pressure ramp, whilst IGR pressure showed a small increase. Prior to the switch to constant pressure the guard ring pressure data showed an increase; IGR pressure peaked at ~5.2 MPa and slowly decayed. This did not correspond with a

change of inflow into, or outflow from, the sample. Up until approximately Day 237, the pressure within the guard rings appeared to be independent of the injection gas pressure. This showed that within the test sample very little pore pressure change had occurred and gas had not started to enter the sample. Even accounting for the differences in compressibility of helium and water, the "bulk" sample pore pressure was relatively unaffected by the injection pressure.

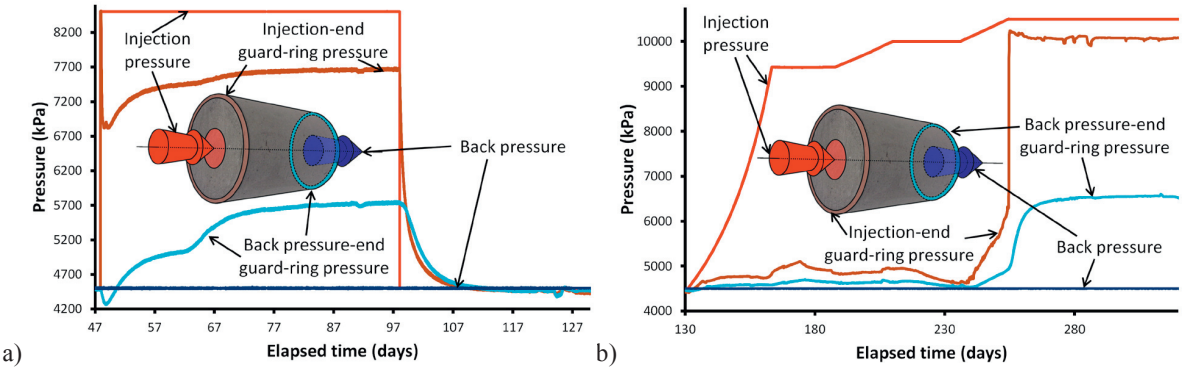

Fig. 1. Results of pore pressure recorded during hydraulic and gas testing of Callovo-Oxfordian claystone; (a) Water-injection testing; (b) Gas injection testing.

The final pressure ramp was initiated on Day 236 and raised pore pressure by 0.5 MPa over a 3 week period; pressure in IGR started to increase from Day 236 onwards. This time represents the onset of gas movement. The observed pore pressure response showed that little change occurred prior to the onset of gas flow. Once gas entry occurred there was a considerable difference in pore pressure within the sample. Pore pressure was not as evenly distributed as was seen during the hydraulic head test. The maximum pressure difference observed equates to a pressure gradient of 400 $MPa.m^{-1}$ and this was stable prior to gas entry.

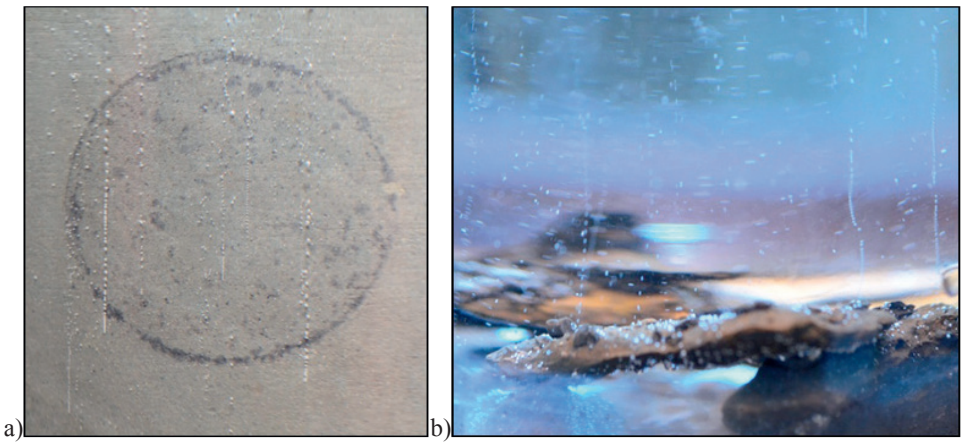

Fig. 2. Observations of gas trapped within claystone released during sample heating in glycerol. (a) Callovo-Oxfordian claystone following gas injection testing; (b) Release of naturally occurring gas from Bowland shale.

The differences between pore pressure response for water and gas flow suggest that the flow mechanisms are different. Tests have shown that at the onset of gas flow Callovo-Oxfordian claystone undergoes volumetric dilation

[9]. This suggests that gas flow was along localized dilatant pathways (micro-fissuring) which may or may not interact with the continuum stress field; also termed dilatancy flow. As well as strain data, dilatancy flow in argillaceous materials has also been suggested from studies of nano-particle invasion in Boom Clay [10] and during the heating of samples in glycerol which suggested that gas flow was through a small number of discrete pathways. Fig. 2a shows the expulsion of gas bubbles from COx following gas injection, whilst Fig. 2b shows the release of shale gas from Bowland shale. In both examples gas pathways occur as a limited number of localized features.

3. Experimental geometry 2 – fracture testing

Three experimental geometries have been used that give insight into fracture transmissivity; the Direct Shear Rig (DSR; [11]), the Angled Shear Rig (ASR; [12]) and Fracture Visualization Rig (FVR; [13]). The DSR was used to investigate fracture transmissivity of Opalinus Clay with normal load of up to 12 MPa, injection pore pressure up to 12 MPa, and controlled shear displacement. Pore fluid was injected directly to the fracture plane between two samples of 60 × 60 × 25 mm by means of a 4 mm diameter injection pipe. The ASR was used to investigate flow within a kaolinite gouge between two steel platens angled to the stress-field. The apparatus was designed with similar specification to the DSR. The FVR was designed to visualize flow paths within a thin clay gouge. The apparatus was made up of a 50 mm thick fused quartz glass “window” of 150 mm diameter. The glass block was constrained by a steel collar that created a normal load of up to 3 MPa. Gas or water was injected at the centre of the steel base plate. Time lapse photography was used to visualize the development of gas pathways within the gouge.

3.1. Observed pore water distribution during fracture testing

Fluorescein was added to the injection fluid towards the end of the test to allow imaging of the distribution of flow along the fracture plane [11]. As shown in Fig. 3a flow was highly variable and far from perfectly radial. Flow preferentially followed micro-scale fractures that formed in the fracture surface. Water flow paths were seen to be complex with only about a half (51.6 %) of the fracture plane contributed to overall flow.

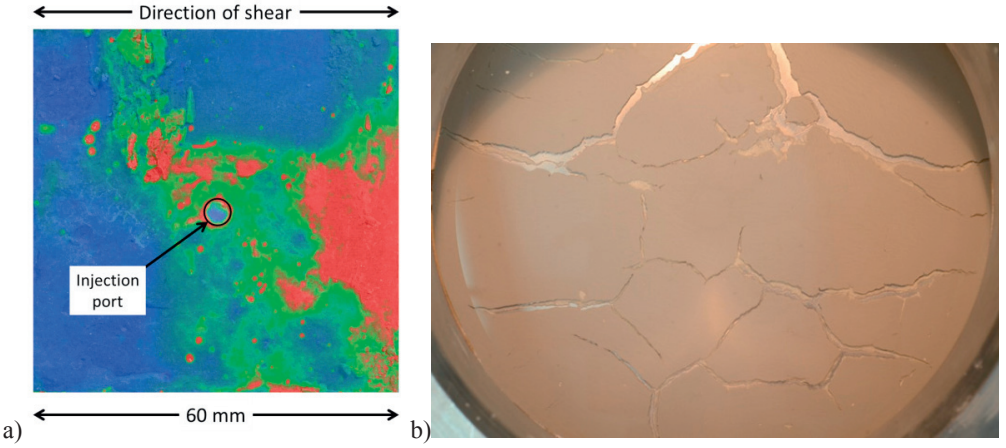

Fig. 3. Observations of fluid flow along fractures. (a) Distribution of fluorescein staining during shear testing of Opalinus Clay. (b) Gas pathway formation in kaolinite paste.

Fig. 4 summarizes fluid flow along a water saturated kaolinite paste using the ASR. Fig. 4a shows the modelled pore pressure distribution expected from a central injection port and radial flow. For hydraulic testing a pore pressure of 1 MPa was used, whereas a pore pressure of 3.5 MPa was necessary to facilitate gas flow. The experimental geometry included two pore pressure sensors in the top block in order to monitor pore pressure within the gouge. As seen in the modelling results (Fig. 4a), the position of these pore pressure sensors predicted a pressure

of 0.3 MPa and 1.1 MPa for the cases of water and gas injection respectively. As seen in Fig. 4b, the observed pore pressure was significantly lower than predicted. For water injection a predicted pressure of 300 kPa corresponds with observed pressures of 80 and 20 kPa. These anisotropic pressures were seen to develop mainly as a result of the compression of the clay gouge. The low pore pressure may suggest that the two pore pressure sensors were located in the 75 % of the fault that was nonconductive, as suggested in Fig. 3a. For gas injection a pore pressure of 1.1 MPa should have been observed, whereas no pore pressure change occurred (Fig. 4b). In both cases it is clear that pore pressure was not a simple radial flow from a central injection point.

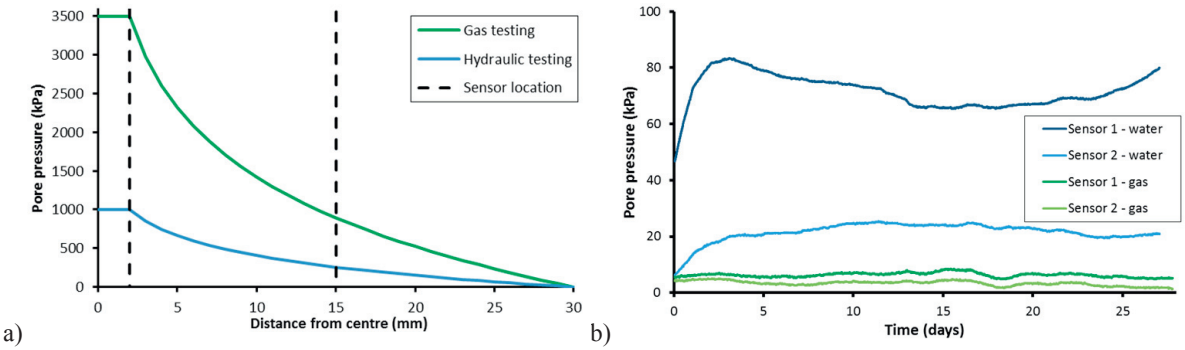

a) b)

Fig. 4. Observations of pore pressure within a kaolinite gouge; (a) Modelled results of predicted pore pressure within the kaolinite gouge; (b) Pore pressure within the gouge during water and gas injection testing.

Fig. 3b shows the results from a gas injection experiment conducted in kaolinite paste using the FVR. As can be clearly seen, gas propagated along a number of localized features, similar in appearance to fractures. Similar distributions of pathways formed during six tests. In all cases, the kaolinite gouge compressed in order to facilitate the formation of the gas pathways. No variation was noted due to increased normal load. Therefore it is clear that gas moves along localized pathways.

4. Experimental geometry 3 – large scale demonstration

The Large scale gas injection test (Lasgit) is a full-scale experiment based on the Swedish KBS-3 radioactive waste disposal repository concept, examining the processes controlling gas and water flow in compact buffer bentonite (see [14]). The experiment was commissioned in a 9 m deep, 1.75 m diameter deposition hole at 420 m depth within the Äspö Hard Rock Laboratory (HRL) in Sweden. Whilst the direct link between this test and unconventional hydrocarbons may not be immediately obvious, the experiment gives insight into how larger volumes of clay-rich material behave. Lasgit has 25 tonnes of pre-compacted bentonite, compared with experiments that may have up to 0.35 kg; therefore Lasgit contains ~1×10^6 more clay than a laboratory experiment.

The Lasgit experiment is highly instrumented and has been continuously running since February 2005. The set-up includes instrumentation to measure total stress, pore-water pressure and relative humidity in 32, 48 and 7 positions respectively.

4.1. Observed pore pressure distribution in large scale testing

The scale of Lasgit has allowed pore pressure to be monitored at 48 locations for in excess of 9 years. Fig. 5a shows the results for a number of pore pressure sensors during the full history of the experiment. Following initial hydration pore pressure at the rock wall increased to between 1,250 and 2,700 kPa and since reaching a maximum around Day 600 had generally decreased. Pore-water pressure within the bentonite blocks had a much more complex history and remained low at 650 – 1,200 kPa, except one sensor that was pressured during the second gas injection test when gas reached that location. The pore pressure history was complex with periods of pressure increase and decrease, with some evidence of seasonal variation.

Whilst the test had been continually hydrated at 2.5 MPa, pore pressure distribution within the deposition hole remained complex ranging from 650 to 2,750 kPa. Hydraulic constant head tests at various times in the test history and psychrometer data from seven locations within the bentonite show that the buffer is in hydraulic disequilibrium. Even taking this into account the distribution of hydraulic pore pressure is complex on the large scale.

Fig. 5b shows the observed pore pressure during a gas injection test (see [14]). Gas pressure was increased at one location to approximately 6 MPa. During this pressurization no other pore pressure sensor showed a change in pore water pressure. At gas breakthrough at Day 1770 pore pressure was seen to change in 6 of the pore pressure sensors on the rock wall (Fig. 5a) with the maximum variation being ~50 kPa, whereas none of the three local pore pressure sensors to the injection point showed no variation.

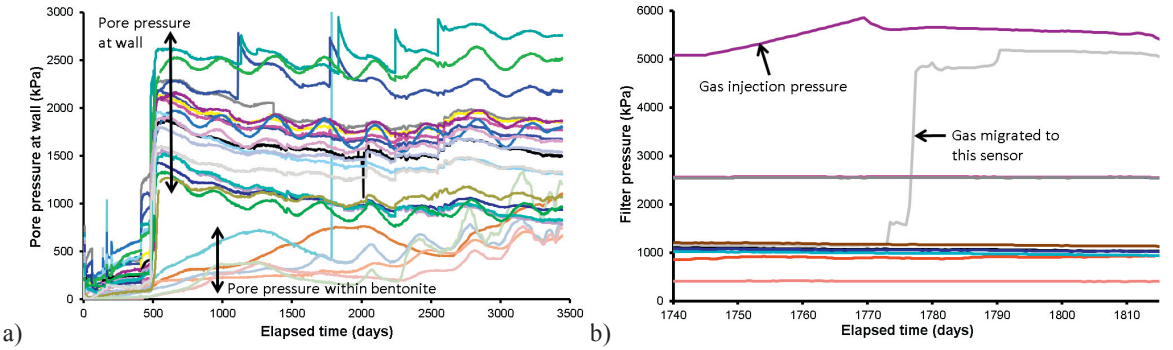

Fig. 5. Hydraulic pore-pressure seen at larger scales; (a) Pore pressure for the entire 9 year history of the Lasgit experiment; (b) pore pressure seen at 9 locations within the buffer during a gas injection test.

Examination of pore pressure sensor data indicates that gas migrated temporally within the system to different locations, as seen in Fig. 5b. Pore pressure at one location (shown grey) started to increase in a series of steps approximately 3 days after gas breakthrough. Pore pressure also greatly increased in one location within the bentonite buffer 15.7 days after gas breakthrough. For both of these events no significant change in pore pressure was observed elsewhere in the system suggesting that gas migrated directly to these sinks. These observations show that gas flow was localized within the bentonite and that pore pressure was heterogeneously distributed.

5. Discussion and implications

The mechanical deformation of argillaceous rocks is usually described in terms of effective stress, which is one of the basic tenets of rock mechanics. In order to do this it is important to accurately describe pore pressure. In this paper we have shown that pore pressure distribution during different laboratory and large-scale experiments was far from simple during both water and gas injection testing. This complexity, even taking into account anisotropy and material heterogeneities, is not easily described by a single value of χ in the law of effective stress as we cannot answer the simple question "what is the pore pressure of the bulk sample?"

Laboratory triaxial experiments suggest that hydraulic pore pressure is not simply dictated by the boundary conditions of the experiment and is complicated by sample heterogeneities. However, the pore pressure distribution observed in shear experiments and on the large scale suggest that pore pressures are not evenly distributed and can be localized into almost isolated areas, although in the case of Lasgit this probably stems from hydraulic disequilibrium. This is most obvious in the shear experimental results where only approximately half of the fracture surface was contributing to the flow of water. Observations within Lasgit show that pore pressure is very heterogeneous, with high pore pressures seen at the rock wall and low pressures seen within the bentonite. Lasgit has demonstrated that disequilibrium lasts for time-scales significantly longer than those experienced during hydraulic fracturing of an unconventional reservoir. This means that induced pore pressure gradients will persist for the duration of production and therefore will affect flow and yield. Constant head testing has no observable effect on

other pore pressure sensors and suggests that pore pressure variation is localized to a relatively small zone around the injection filter.

The observations of pore pressure variation during gas injection show that gas transport mechanisms are dissimilar to water flow. Pore pressure observations consistently show localized increases in pore pressure with gas flow along a number of potentially isolated dilatant pathways (micro-fissures). These observations suggest that under these circumstances a meaningful average pore pressure could be difficult to define. Gas pressure within the micro-fissure pathway can be greater than the pore pressure in the clay surrounding the pathway. A certain amount of pore pressure increase and pore water displacement will occur close to the pathway as a combination of dilation, which will result in localized compression of the clay material, increasing pore pressure through compression of the micro-fissure wall, and the transmission of gas pressure directly through the pathway wall due to the loss of capillary pressure. The driving force of micro-fissure propagation is the gas pressure at the tip of the dilatant feature, which is much greater than the "bulk" pore pressure of the sample. As seen in Lasgit, the majority of the system sees no change in pore pressure as gas pressure increases in an injection filter and even when gas becomes mobile and enters the buffer the pore pressure in the greater part of the system does not vary. Individual sensor responses in triaxial and full-scale testing show that argillaceous materials see no change in pore pressure until gas migrates near to that location and that pressure build-up is then seen to develop quickly.

Consistent behavior is observed in a range of argillaceous materials for different experimental geometries; including triaxial (Callovo-Oxfordian claystone), interface (kaolinite), shear (Opalinus Clay) and large-scale testing (bentonite). This suggests a commonality of behavior independent of experimental setup and a common underlying physical mechanism involved in gas and water flow. Only relatively minor differences are observed between argillaceous materials, which may be explained by differences in material properties, state of induration, and the degree of heterogeneity.

The experimental observations have a number of implications for understanding the extraction of unconventional hydrocarbons. Modelling of the system usually includes the assumption that the material follows the effective stress law. Despite being a porous material, the presented results show that clay-rich materials do not behave as perfectly porous media. Pore pressure is not always transmitted as expected and this is due to material heterogeneity, localization of flow, drainage effects in such low permeability rocks, and the degree of saturation. Therefore classical models of rock deformation will not fully describe the pore pressure effect. In terms of enhanced gas pressure, the transmission of pore pressure is highly localized and large stable pore pressure gradients are able to be sustained for operational time-scales. Many of the observed experimental features suggest highly localized increases in pore pressure and a heterogeneous pore pressure distribution. These observations support the hypothesis of dilatancy flow along micro-fissures being the dominant physical mechanism controlling gas flow. Therefore on a micro scale the law of effective stress will describe the deformation of the clay matrix, but on a bulk scale care has to be taken as the "bulk" pore pressure may vary considerably depending on the number, geometry and distribution of gas pathways.

The fracturing process will result in a number of discrete features. The flow along these will be localized in the case of gas flow or restricted for water flow, with only a proportion of the fracture surface conductive to flow. This highlights the importance of the use of propants in order to facilitate more of the fracture to be conductive for prolonged periods of time.

The release of gas within shale is dependent on a number of factors. The pervasive fracturing of the material results in connectivity of the free gas trapped within the pore space of the rock. However, significant quantities of gas are retained in the clay-rich material between the fractures. The release of this gas requires a change in pore pressure to drive gas movement, which will occur through localized pathways. The experimental observations suggest that a pervasive lowering of pore pressure may have a limited effect away from fractures, meaning that a large proportion of gas remains trapped within pore space and sorbed onto mineral surfaces.

6. Conclusions

Large, stable pressure differentials and gradients were observed in several argillaceous materials during water and gas injection testing for a number of experimental geometries, including triaxial (Callovo-Oxfordian claystone), shear (kaolinite and Opalinus Clay) and full-scale testing (bentonite). Pore-pressure during water injection appeared

to be evenly distributed on the sample scale, although this was complicated by sample heterogeneities. In large scale testing a complex distribution was seen, which may partly be due to hydraulic disequilibrium. During gas injection testing all observations suggested that transport was predominantly by dilatancy flow and the formation of micro-fissures. This led to localized pore pressure variations and a complex temporally and spatially varying pore pressure distribution. Isolated pockets of increased gas pressure could be seen to be stable.

The nature of pore-pressure distribution, both hydraulic and gaseous, and the stability of pore pressure differentials means that the description of a meaningful average pore pressure was difficult and thus the use of effective stress with a single χ value might misrepresent local stresses within the sample. Localized deformation in the formation of dilatant pathways was dominated by the local gas pressure and not the bulk pore pressure. Therefore the law of effective stress on the micro-scale will be valid, whereas on a bulk scale could lead to errors in model predictions. The experimental observations suggest that a pervasive lowering of pore pressure may have a limited effect away from fractures, meaning that a large proportion of gas remains trapped within pore space and sorbed onto mineral surfaces. This has important implications for gas recovery and therefore the economic viability of a shale play.

Acknowledgements

This study was undertaken by staff from the British Geological Survey and is published with the permission of the Executive Director, British Geological Survey (NERC).

References

[1] Cuss RJ, Harrington JF, Graham CJ, Sathar S, Milodowski T. Observations of stable high-pressure differentials in clay-rich materials; implications for the concept of effective stress. *Mineral Mag* 2012; 76(8): pp.3115-3129

[2] Hubbert MK, Rubey WW. Role of fluid pressure in mechanics of overthrust faulting: 1 - Mechanics of fluid-filled porous solids and its application to overthrust faulting. *Geol Soc Am Bull* 1959; 70: pp. 115-166.

[3] Terzaghi K. *Theoretical Soil Mechanics*. New York, John Wiley; 1943.

[4] Handin J, Hager RV, Friedman M, Feather JN. Experimental deformation of sedimentary rocks under confining pressure; pore pressure tests. *Bull Am Assoc Petrol Geol* 1963; 47: pp. 717-755.

[5] Kwon O, Kronenberg AK, Gangi AF, Johnson B. Permeability of Wilcox Shale and its effective pressure law. *J Geophys Res* 2001; 106: pp. 19,339-19,353.

[6] Biot MA. General theory of three-dimensional consolidation. *J Appl Phys* 1941; 12: pp. 155-164.

[7] Burrus J. Overpressure models for clastic rocks, their relation to hydrocarbon expulsion: A critical re-evaluation, in BE Law, GF Ulmishek, VI Slavin eds. *Abnormal pressures in hydrocarbon environments*. AAPG Memoir 70; 1998: p. 35-63.

[8] Schofield A, Wroth CP. *Critical State Soil Mechanics*. London, McGraw-Hill; 1968: 310 pp.

[9] Cuss RJ, Harrington J, Giot R, Auvray C. Experimental observations of mechanical dilation at the onset of gas flow in Callovo-Oxfordian claystone. *Clays in Natural and Engineered Barriers for Radioactive Waste Confinement*. 400: Geological Society Special Publications: London, United Kingdom, Geological Society of London; 2014.

[10] Harrington JF, Milodowski AE, Graham CC, Rushton JC, Cuss RJ. Evidence for gas-induced pathways in clay using a nanoparticle injection technique. *Mineral Mag* 2012; 76(8): pp.3327-3336.

[11] Cuss RJ, Milodowski A, Harrington JF. Fracture transmissivity as a function of normal and shear stress: first results in Opalinus clay. *Phys Chem Earth* 2011; 36: pp.1960-1971.

[12] Sathar S, Reeves HJ, Cuss RJ, Harrington JF. Critical stress theory applied to repository concepts; the importance of stress tensor and stress history in fracture flow. *Mineral Mag* 2012; 76(8): pp.3165-3177.

[13] Wiseall A, Cuss RJ, Harrington JF, Graham CC. *The visualisation of flow-paths in experimental studies of clay-rich rocks*. IGD-TP Geodisposal 2014. 24th – 26th June 2014, Manchester, UK.

[14] Cuss RJ, Harrington JF, Noy DJ, Wikman A, Sellin P. Large scale gas injection test (Lasgit): Results from two gas injection tests. *Phys Chem Earth* 2011; 36: pp.1729-1742.